# A study of the singlet–triplet perturbations in the $\tilde{A}\ ^1A_u$ state of acetylene by high resolution ultraviolet spectroscopy

Marcel Drabbels, Johannes Heinze,[a] and W. Leo Meerts
*Department of Molecular and Laser Physics, University of Nijmegen, Toernooiveld, 6525 ED Nijmegen, The Netherlands*

(Received 13 August 1993; accepted 9 September 1993)

Laser-induced fluorescence spectra of the $3_0^3\,K_0^1$ and $3_0^4\,K_0^1$ vibronic bands of the $\tilde{A}\ ^1A_u \leftarrow \tilde{X}\ ^1\Sigma_g^+$ transition in acetylene have been recorded with a resolution of 18 MHz. Each rotational transition consists of a group of lines due to coupling of the electronically excited singlet state with isoenergetic triplet states. Using the standard deconvolution procedure the singlet–triplet coupling elements and the density of coupled triplet states are derived for rotational levels up to $J=4$ in both bands. From the density of coupled triplet states it is concluded that the $\tilde{A}\ ^1A_u$ state is perturbed by the $T_1\ ^3B_2$ state. Magnetic field measurements have shown that the predissociation of acetylene in the $4\nu_3'$ vibrational level of the $\tilde{A}$ state is caused by a coupling via the $T_1\ ^3B_2$ state with predissociating vibrational levels of the electronic ground state.

## I. INTRODUCTION

Acetylene plays an important role in bridging the gap between diatomic and large polyatomic molecules and is therefore one of the most intensively studied small polyatomic species. The $\tilde{A}\ ^1A_u \leftarrow \tilde{X}\ ^1\Sigma_g^+$ band system of acetylene has been well analyzed spectroscopically.[1–5] On the basis of these studies it was concluded that acetylene has a *trans*-bent geometrical structure in the electronically excited $\tilde{A}$ state, in contrast to the linear structure in the electronic ground state. A laser-induced fluorescence (LIF) study by Schrerer *et al.*[6] showed that the rotational structure of the $\tilde{A}\ 3\nu_3'$ vibrational level is strongly perturbed. An extensive analysis of the perturbation showed that it arises from a Fermi interaction between the $3\nu_3'$ and the $\nu_2' + 2\nu_4'$ vibrational levels. The observation of quantum beats in other LIF studies indicated that this level is also perturbed by other interactions.[7] A study of these quantum beat phenomena in the presence of a magnetic field revealed that the $3\nu_3'$ level is perturbed by a singlet–triplet interaction.[8,9] Recently, extensive studies on this singlet–triplet interaction in the vibronic levels of the $\tilde{A}$ state were reported by Dupre *et al.*[10] and by Ochi and Tsuchiya.[11] Both experiments not only showed that a strong interaction ($\sim$GHz) is present between the rovibronic levels of the $\tilde{A}$ state and isoenergetic triplet states but also showed the existence of a weak coupling ($\sim$MHz) between triplet states and high-lying vibrational levels of the electronic ground state.

In the present experiment we have recorded the LIF spectrum of the $3_0^3\,K_0^1$ and $3_0^4\,K_0^1$ vibronic bands of the $\tilde{A}\ ^1A_u \leftarrow \tilde{X}\ ^1\Sigma_g^+$ transition in acetylene with a resolution of 18 MHz. This resolution is sufficient to resolve the splitting of rotational lines due to the singlet–triplet interactions. Using the standard deconvolution procedure the coupling elements and the density of coupled triplet states can be obtained from the recorded spectra, giving information on the coupling mechanism and the identity of the coupled triplet state.

## II. EXPERIMENT

The laser system and molecular beam apparatus have been extensively described before.[12] Therefore, only the relevant features will be given here. The laser system consists of a single-frequency cw ring dye laser (Spectra Physics 380D) which is operated with Stilbene 3 dye and is pumped by an Argon ion laser (Spectra Physics 2045-15) with a maximum UV output of 7 W. For the generation of narrow bandwidth UV radiation in the wavelength range of 213–225 nm, an angle-tuned $\beta$-$BaB_2O_4$ (BBO) crystal is placed in the auxiliary beam waist of the laser cavity. Due to the nonlinear properties of the crystal, UV radiation is generated at the second harmonic of the fundamental laser frequency. In order to minimize the losses in the laser cavity the crystal is placed at Brewster angle. In this way UV radiation with a bandwidth of less than 1 MHz and a power up to 150 $\mu$W is obtained. For relative frequency calibration the transmission fringes of a temperature and pressure stabilized Fabry–Perot interferometer with a free spectral range of 149.72 MHz are recorded along with the excitation spectrum. For absolute frequency calibration the absorption spectrum of the $Te_2$ molecule[13] at the fundamental laser frequency is recorded.

The molecular beam is formed by a continuous expansion of pure acetylene or acetylene seeded in argon through a nozzle with a diameter of 100 $\mu$m. The backing pressure applied is typically 1 atm. The rotational temperature in the molecular beam was found to vary between 3 and 9 K depending on the acetylene concentration. The molecular beam is skimmed twice and enters a differential pumped LIF detection chamber about 30 cm downstream of the nozzle. The molecular beam is at that point crossed per-

[a]Present address: Deutsche Forschungsanstalt für Luft- und Raumfahrt, Forschungszentrum Stuttgart, W-7000 Stuttgart 80, Germany.

 0021-9606/94/100(1)/165/10/$6.00  

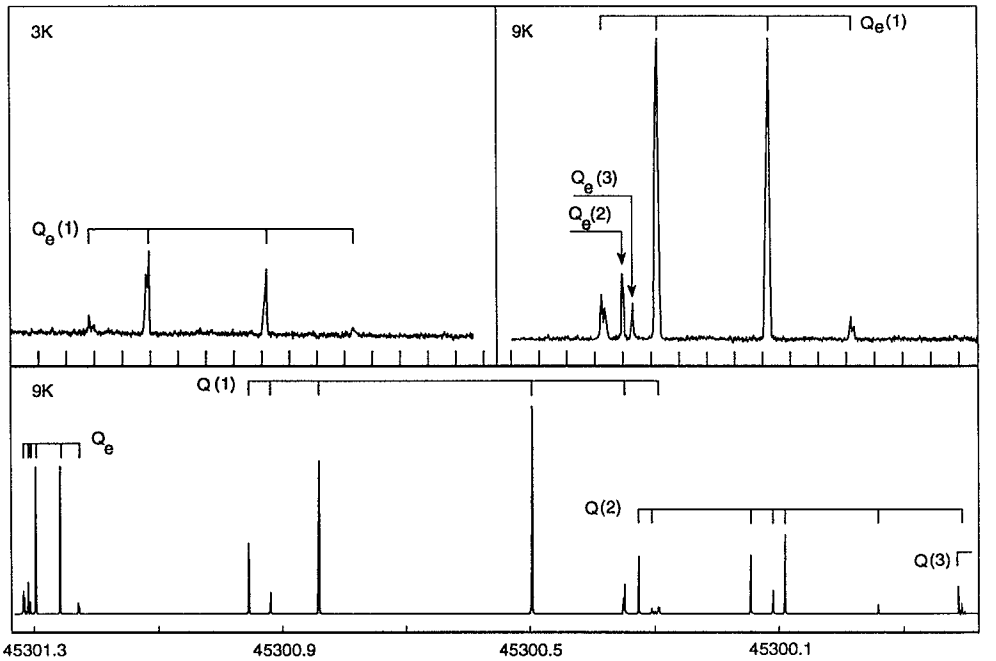


FIG. 1. Lower panel: $Q$ branch of the $3_0^3 K_0^1$ vibronic band of the $\tilde{A}\,^1A_u \leftarrow \tilde{X}\,^1\Sigma_g^+$ electronic transition in acetylene recorded at an estimated rotational temperature of 9 K. Upper panel: Recording of the $Q_e$ branch at rotational temperatures of 3 K (left part) and 9 K (right part). The frequency is marked every 300 MHz and increases from right to left.

pendicularly by the weakly focused UV laser beam which resonantly excites the molecules from the electronic ground state $\tilde{X}\,^1\Sigma_g^+$ to the $\tilde{A}\,^1A_u(\nu_3' = 3,4)$ state. The laser-induced fluorescence is collected by two spherical mirrors and imaged onto a photomultiplier. The linewidth of the individual transitions in the recorded LIF spectra amounts to 18 MHz. This linewidth is mainly determined by the residual Doppler width in the molecular beam in combination with the spatial sensitivity of the collection optics.

For measurements in a magnetic field a pair of coils in a non-Helmholtz configuration are mounted. With this setup it is possible to generate magnetic fields up to 100 Gauss with an accuracy of 5%. The direction of the magnetic field is parallel the laser beam.

## III. RESULTS AND DISCUSSION

Two vibronic bands of the $\tilde{A}\,^1A_u \leftarrow \tilde{X}\,^1\Sigma_g^+$ transition in acetylene have been recorded at high resolution, i.e., the $3_0^3 K_0^1$ band at 221 nm and the $3_0^4 K_0^1$ band at 216 nm. Each band consists of a $P$, $Q$, and $R$ branch, characteristic for a $\Delta K = 1$ transition. Figure 1 shows a part of the $Q$ branch of the $3_0^3 K_0^1$ band recorded at different temperatures.

It can directly be seen that this band is strongly perturbed since each rotational line is split into a large number of lines. The same conclusion is valid for the $3_0^4 K_0^1$ band. It has been well established that the rotational levels in both bands are perturbed by a strong interaction with isoenergetic triplet states.[9–11] The observed line positions and their assignments are given in Table I. The rotational assignment for the $P$ and $R$ transitions has been verified by comparison of the $P$- and $R$-branch combination differences to the well-known ground state combination differences.[14] The $P$ transitions have not been incorporated in this table since they give no substantial new information. The frequencies of the $P$ transitions can easily be calculated from the reported $R$ transitions and the well-known ground state constants.[14] The assignment for the $Q$ lines cannot be verified by combination differences. The assignment of these lines has been checked by comparing the intensities of the different lines at various rotational temperatures.

### A. Fermi perturbation

From the low resolution work of Scherer *et al.*,[6] it is known that the $3\nu_3'$ level in the $\tilde{A}$ state is perturbed, most probably by a Fermi interaction with the $\nu_2' + 2\nu_4'$ vibrational level. All the so-called "extra" $P_e$, $Q_e$, and $R_e$ transitions induced by this perturbation that were observed by Scherer *et al.* are also observed in the present high resolution study and most of them consist of several lines, see Table I. The high resolution spectra confirm the previous assignments of the $P_e$ and $R_e$ transitions. However, for the $Q_e$ transitions the assignment has to be revised. The transition previously assigned as "extra" $Q_e(1)$ appears to consist of several lines that involve transitions from higher rotational levels, as can be seen in Fig. 1. On the basis of the temperature dependence of the intensities of these lines they are assigned to $Q_e(2)$ and $Q_e(3)$ transitions. On the same basis it has to be concluded that the transition previously assigned as "extra" $Q_e(2)$ consists of lines belonging to the $Q(1)$ transition. Another indication that these lines belong to the $Q(1)$ transition is provided by the fact that some of the lines show a hyperfine splitting, which can only be present in $Q$ transitions involving odd $J$ levels, see Sec. III C.

TABLE I. Transition frequency ($cm^-$), amount of $\tilde{A}\,^1A_u$ state character, $|C_s|^2$, singlet–triplet coupling matrix elements, $V_{ST}$, (MHz), effective Fermi contact parameter, $A_{eff}$, (MHz) and the gyromagnetic factor, $g_{eff}$, of the individual molecular eigenstates as obtained from the study of the $\tilde{A}\,^1A_u \leftarrow \tilde{X}\,^1\Sigma_g^+$ system.

| Transition | | Freq.[a] | $\lvert C_s\rvert^2$ | $V_{st}$[b] | $A_{eff}$[c] | $\lvert g_{eff}\rvert$[d] | $\frac{A_{eff}}{\lvert g_{eff}\rvert}$ |
|---|---|---|---|---|---|---|---|
| $3_0^3K_0^1$ | $R(0)$ | 45 302.7299 | 0.02 | 489 | – | <0.05 | – |
| | | 2.7397 | 0.04 | 1873 | – | 0.48 | – |
| | | 2.7866 | 0.04 | 2561 | – | 0.34 | – |
| | | 2.9032 | 0.06 | 2574 | – | 1.06 | – |
| | | 3.1653 | 0.48 | – | – | 0.47 | – |
| | | 3.2120 | 0.36 | 752 | – | 0.60 | – |
| | $R_e(0)$ | 45 303.5710 | 0.09 | 958 | – | <0.05 | – |
| | | 3.6518 | 0.01 | 1 | – | 1.95 | – |
| | | 3.6820 | 0.90 | – | – | 0.15 | – |
| | $Q(1)$ | 45 300.3134 | 0.02 | 824 | 17.3 | 1.18 | 14.6 |
| | | 0.3650 | 0.08 | 1905 | 18.7 | 1.08 | 17.3 |
| | | 0.5172 | 0.48 | – | 9.7 | 0.56 | 17.3 |
| | | 0.8335 | 0.26 | 5152 | 11.0 | 0.88 | 12.5 |
| | | 0.9102 | 0.04 | 1586 | < | <0.05 | – |
| | | 0.9458 | 0.12 | 1328 | < | 0.16 | – |
| | $Q_e(1)$ | 45 301.2420 | 0.04 | 324 | 12.0 | 0.77 | 15.6 |
| | | 1.2839 | 0.40 | 524 | < | <0.05 | – |
| | | 1.3168 | 0.45 | – | 5.0 | 0.22 | 22.6 |
| | | 1.3407 | 0.12 | 313 | 16.5 | 0.93 | 17.8 |
| | $R(1)$ | 45 304.9428 | 0.06 | 1499 | 15.0 | 0.80 | 18.8 |
| | | 4.9993 | 0.06 | 1759 | 15.0 | 0.80 | 18.8 |
| | | 5.0713 | 0.06 | 1301 | < | 0.22 | – |
| | | 5.1113 | 0.05 | 1603 | < | <0.05 | – |
| | | 5.1848 | 0.06 | 722 | 15.0 | 0.84 | 17.8 |
| | | 5.2140 | 0.07 | 426 | < | 0.11 | – |
| | | 5.2272 | 0.10 | 846 | 3.6 | 0.38 | |
| | | 5.2630 | 0.24 | – | 6.0 | 0.43 | 14.0 |
| | | 5.3239 | 0.14 | 1282 | < | <0.05 | – |
| | | 5.3583 | 0.16 | 844 | 2.0 | 0.16 | 12.5 |
| | $R_e(1)$ | 45 305.9406 | 0.07 | 387 | 10.0 | – | – |
| | | 5.9905 | 0.93 | – | < | 0.09 | – |
| | $Q(2)$ | 45 299.8147 | 0.04 | 2037 | – | 0.55 | – |
| | | 9.9587 | 0.04 | 1257 | – | <0.05 | – |
| | | 0.1139 | 0.33 | – | – | 0.33 | – |
| | | 0.1325 | 0.09 | 412 | – | <0.05 | – |
| | | 0.1649 | 0.26 | 713 | – | <0.05 | – |
| | | 0.3257 | 0.02 | 441 | – | <0.05 | – |
| | | 0.3464 | 0.23 | 2740 | – | 0.16 | – |
| | $Q_e(2)$ | 45 301.3277 | 1.00 | – | – | <0.05 | – |
| | $R(2)$ | 45 306.9844 | 0.03 | 503 | – | <0.03 | – |
| | | 6.9966 | 0.03 | 929 | – | 0.28 | – |
| | | 7.0591 | 0.02 | 193 | – | – | – |
| | | 7.0849 | 0.49 | – | – | 0.16 | – |
| | | 7.1411 | 0.01 | 412 | – | 0.08 | – |
| | | 7.2983 | 0.30 | 3238 | – | 0.43 | – |
| | | 7.3190 | 0.03 | 311 | – | 0.25 | – |
| | | 7.3439 | 0.06 | 704 | – | 0.10 | – |
| | | 7.3497 | 0.03 | 209 | – | 0.04 | – |
| | $R_e(2)$ | 45 308.3830 | 1.00 | – | – | – | – |
| | $Q(3)$ | 45 298.8097 | 0.04 | 3672 | 10.3 | 0.58 | 17.6 |
| | | 8.9228 | 0.01 | 1702 | < | – | – |
| | | 9.2587 | 0.01 | 494 | < | 0.20 | – |
| | | 9.3149 | 0.01 | 340 | < | <0.05 | – |
| | | 9.3890 | 0.16 | 674 | 6.2 | 0.31 | 19.6 |
| | | 9.4385 | 0.59 | – | < | <0.05 | – |
| | | 9.4612 | 0.02 | 135 | < | 0.18 | – |
| | | 9.4785 | 0.03 | 276 | < | 0.11 | – |
| | | 9.6334 | 0.05 | 1848 | < | 0.26 | – |
| | | 9.6826 | 0.03 | 1374 | < | 0.43 | – |
| | | 9.6971 | 0.01 | 482 | < | – | – |
| | | 9.8200 | 0.06 | 2452 | < | 0.05 | – |
| | $Q_e(3)$ | 45 301.3315 | 1.00 | – | ~3 | <0.05 | – |
| | $R(3)$ | 45 308.5101 | 0.02 | 1016 | < | – | – |
| | | 8.5245 | 0.01 | 1734 | < | – | – |
| | | 8.7110 | 0.01 | 278 | < | 0.20 | – |
| | | 8.7493 | 0.02 | 290 | < | 0.29 | – |
| | | 8.7802 | 0.33 | – | < | 0.19 | – |
| | | 8.8397 | 0.08 | 1341 | < | 0.13 | – |
| | | 8.8507 | 0.02 | 378 | < | 0.26 | – |
| | | 8.9261 | 0.09 | 1340 | < | 0.30 | – |
| | | 8.9772 | 0.22 | 2312 | < | 0.20 | – |
| | | 9.0454 | 0.06 | 1301 | 5.5 | 0.37 | 14.9 |
| | | 9.0744 | 0.05 | 860 | 12.3 | 0.82 | 15.0 |
| | | 9.1786 | 0.01 | 556 | < | 0.34 | – |
| | | 9.2206 | 0.01 | 984 | < | 0.24 | – |
| | | 9.2512 | 0.02 | 3268 | < | 0.17 | – |
| | | 9.3231 | 0.06 | 34 | 11.6 | 0.70 | – |
| | $Q(4)$ | 45 297.9482 | 0.03 | 2635 | – | – | – |
| | | 8.1892 | 0.03 | 922 | – | – | – |
| | | 8.2319 | 0.10 | 2828 | – | – | – |
| | | 8.3930 | 0.04 | 498 | – | – | – |
| | | 8.4096 | 0.07 | 1136 | – | – | – |
| | | 8.4716 | 0.21 | 600 | – | – | – |
| | | 8.4975 | 0.20 | 2823 | – | – | – |
| | | 8.6582 | 0.28 | – | – | – | – |
| | | 8.6998 | 0.04 | 558 | – | – | – |
| $3_0^4K_0^1$ | $R(0)$ | 46 290.1903 | 0.01 | 698 | – | – | – |
| | | 0.3278 | 0.14 | 597 | – | 0.05 | – |
| | | 0.3563 | 0.25 | 2289 | – | 0.17 | – |
| | | 0.5047 | 0.58 | – | – | 0.23 | – |
| | | 0.5346 | 0.08 | 121 | – | – | – |
| | | 0.7135 | 0.08 | 673 | – | – | – |
| | $Q(1)$ | 46 287.7308 | 0.01 | 399 | < | – | – |
| | | 7.9211 | 0.50 | – | < | 0.19 | – |
| | | 8.0625 | 0.46 | 2154 | 9.3 | 0.37 | 25.1 |
| | | 8.2089 | 0.01 | 712 | 19.0 | – | – |
| | | 8.2958 | 0.02 | 1152 | 19.0 | – | – |
| | $R(1)$ | 46 292.2675 | 0.01 | 629 | < | – | – |
| | | 2.2932 | 0.01 | 695 | < | – | – |
| | | 2.4368 | 0.20 | 914 | 7.2 | 0.23 | 31.3 |
| | | 2.4880 | 0.23 | 704 | < | 0.19 | – |
| | | 2.5202 | 0.19 | 711 | 6.4 | 0.31 | 20.6 |
| | | 2.5562 | 0.36 | – | < | 0.06 | – |
| | $Q(2)$ | 46 287.2059 | 0.06 | 1970 | – | – | – |
| | | 7.2690 | 0.02 | 1143 | – | – | – |
| | | 7.3156 | 0.01 | 701 | – | – | – |
| | | 7.3345 | 0.01 | 372 | – | – | – |
| | | 7.3384 | 0.01 | 898 | – | – | – |
| | | 7.4782 | 0.01 | 143 | – | – | – |
| | | 7.5145 | 0.76 | – | – | 0.02 | – |
| | | 7.5298 | 0.01 | 100 | – | – | – |
| | | 7.6395 | 0.12 | 1290 | – | 0.41 | – |
| | $R(2)$ | 46 294.0436 | 0.01 | 770 | – | – | – |
| | | 4.2301 | 0.02 | 449 | – | – | – |

TABLE I. (*Continued.*)

| Transition | Freq.[a] | $\lvert C_s\rvert^2$ | $V_{st}$[b] | $A_{\text{eff}}$[c] | $\lvert g_{\text{eff}}\rvert$[d] | $\frac{A_{\text{eff}}}{\lvert g_{\text{eff}}\rvert}$ |
|---|---|---|---|---|---|---|
| | 4.2966 | 0.32 | – | – | 0.48 | – |
| | 4.3450 | 0.09 | 765 | – | 0.06 | – |
| | 4.3802 | 0.21 | 1089 | – | 0.05 | – |
| | 4.3970 | 0.26 | 362 | – | 0.08 | – |
| | 4.4798 | 0.05 | 783 | – | 0.63 | – |
| | 4.6158 | 0.01 | 939 | – | – | – |
| | 4.7296 | 0.01 | 1328 | – | – | – |
| | 4.7965 | 0.01 | 1176 | – | – | – |
| $Q(3)$ | 46 286.5354 | 0.07 | 1549 | 7.7 | 0.31 | 24.8 |
| | 6.6016 | 0.02 | 723 | < | 0.15 | – |
| | 6.6641 | 0.11 | 734 | < | 0.06 | – |
| | 6.6809 | 0.01 | 325 | < | 0.12 | – |
| | 6.6914 | 0.08 | 1093 | < | 0.15 | – |
| | 6.7310 | 0.11 | 1205 | < | <0.02 | – |
| | 6.7951 | 0.23 | – | 4.9 | 0.25 | 19.6 |
| | 6.8069 | 0.17 | 274 | 5.7 | 0.19 | 30.0 |
| | 6.8220 | 0.07 | 307 | 8.2 | 0.22 | 37.3 |
| | 6.8557 | 0.10 | 661 | 14.7 | 0.58 | 25.3 |
| | 6.9875 | 0.01 | 754 | < | – | – |
| | 7.1287 | 0.03 | 1670 | 18.0 | – | – |
| $R(3)$ | 46 296.0003 | 0.42 | – | 6.6 | 0.39 | |
| | 6.0747 | 0.28 | 1318 | 3.3 | 0.17 | 19.4 |
| | 6.0977 | 0.05 | 387 | < | <0.03 | – |
| | 6.1135 | 0.02 | 310 | < | 0.06 | – |
| | 6.1851 | 0.15 | 1612 | 8.4 | 0.40 | 21.0 |
| | 6.2839 | 0.01 | 541 | 9.8 | – | – |
| | 6.3366 | 0.01 | 816 | 12.8 | – | – |
| | 6.4175 | 0.09 | 2796 | < | 0.30 | – |
| $Q(4)$ | 46 285.5305 | 0.02 | 214 | – | – | – |
| | 5.5463 | 0.12 | 540 | – | 0.14 | – |
| | 5.5608 | 0.01 | 239 | – | – | – |
| | 5.6009 | 0.69 | | – | <0.02 | – |
| | 5.6143 | 0.02 | 86 | – | – | – |
| | 5.6270 | 0.12 | 285 | – | 0.19 | – |
| | 5.6428 | 0.02 | 153 | – | – | – |

[a]The relative accuracy in the line positions is 0.0005 $cm^{-1}$. The absolute accuracy is 0.002 $cm^{-1}$.
[b]The coupling matrix elements given at a molecular eigenstate correspond to the interaction strength between the zero-order singlet level and the triplet state having the largest contribution to the molecular eigenstate.
[c]The error in the effective Fermi contact parameter is 10%. –indicates no hyperfine structure present, < indicates hyperfine structure not observable.
[d]The error in gyromagnetic factor is 10% for states having no hyperfine structure and 20% for states having hyperfine structure.

It has been pointed out by Scherer *et al.*[6] that it is very unlikely that the observed "extra" lines are due to transitions to a hitherto unobserved singlet state or due to transition to triplet states. Consequently, it has to be assumed that the "extra" transitions arise from a Fermi interaction of the $3\nu_3'$ level with another vibrational level of the $\tilde{A}$ state, most probably the $\nu_2' + 2\nu_4'$ combination band. In order to analyze this Fermi perturbation it is necessary to know the energy levels of the unperturbed singlet states. We therefore have determined the center of gravity of lines in the excitation spectrum belonging to the same rotational transition. The line positions of the singlet levels can be found in Table II. These line positions of both the $3\nu_3'$ state and

TABLE II. Calculated transition frequencies of zero-order singlet states ($cm^{-1}$), the average singlet–triplet coupling matrix elements, $\langle V_{ST}\rangle$, (MHz) and the density of coupled triplet states, $\rho_T$, (states/$cm^{-1}$) for the observed transitions.

| Vibr. level | Trans. | Freq. $\lvert S_1\rangle$ | $\langle V_{ST}\rangle$ | $\rho_T$ |
|---|---|---|---|---|
| $3\nu_3'$ | $R(0)$ | 45 302.1277 | 1653 | 8.7 |
| | $R(1)$ | 45 305.2192 | 1142 | 20.6 |
| | $R(2)$ | 45 307.1762 | 812 | 19.4 |
| | $R(3)$ | 45 308.9112 | 1124 | 16.1 |
| | $Q(1)$ | 45 300.6482 | 2159 | 6.6 |
| | $Q(2)$ | 45 300.1657 | 1267 | 10.0 |
| | $Q(3)$ | 45 299.4453 | 1219 | 10.4 |
| | $Q(4)$ | 45 298.4806 | 1500 | 9.6 |
| $\nu_2'+2\nu_4'$ | $R_e(0)$ | 45 303.6698 | 479 | 19.0 |
| | $R_e(1)$ | 45 305.9893 | 387 | – |
| | $R_e(2)$ | 45 308.3830 | – | – |
| | $Q_e(1)$ | 45 301.3038 | 387 | 21.5 |
| | $Q_e(2)$ | 45 301.3277 | – | – |
| | $Q_e(3)$ | 45 301.3315 | – | – |
| $4\nu_3'$ | $R(0)$ | 46 290.4412 | 876 | 7.7 |
| | $R(1)$ | 46 292.5046 | 731 | 15.0 |
| | $R(2)$ | 46 294.3663 | 851 | 10.7 |
| | $R(3)$ | 46 296.0949 | 1111 | 17.3 |
| | $Q(1)$ | 46 287.9963 | 1104 | 5.4 |
| | $Q(2)$ | 46 287.5014 | 827 | 17.5 |
| | $Q(3)$ | 46 286.7662 | 845 | 17.5 |
| | $Q(4)$ | 46 285.5971 | 253 | 45.3 |

perturbing state have been fit to an effective Hamiltonian as described by Scherer *et al.*[6] In the least squares fit the rotational constants of the ground state were kept fixed at the accurate values determined by infrared spectroscopy.[14] Since there are insufficient data to determine the $A'$ rotational constants we decided to determine the effective term values. It turned out the Fermi interaction parameter could not be determined from the observed data, indicating that the model used is not correct. Analysis in terms of a Coriolis interaction did not improve the situation. Using constrained values for the Fermi interaction parameter showed that the best fit resulted when the interaction strength was set equal to zero. The molecular constants obtained from the fit with the interaction strength set to zero are listed in Table III. The standard deviation of the fit is about 0.02 $cm^{-1}$. In view of the interval of 0.5 $cm^{-1}$ over which the lines belonging to the same rotational transition extends, the fit is quite satisfactory. For comparison the constants for the $4\nu_3'$ level are also given.

The rotational constants found for the $3\nu_3'$ and $4\nu_3'$ levels agree to a reasonable extent with former studies.[3,4,6] The constants of the perturbing state, however, differ

TABLE III. Molecular constants ($cm^{-1}$) of three vibrational levels in the $\tilde{A}\,^1A_u$ state of acetylene.

| | $3\nu_3'$ | $\nu_2'+2\nu_4'$ | $4\nu_3'$ |
|---|---|---|---|
| $B'$ | 1.031(2) | 1.178(3) | 1.017(3) |
| $C'$ | 1.131(2) | 1.179(3) | 1.125(2) |
| $T_0$ | 45 300.90(3) | 45 301.30(3) | 46 288.26(3) |

strongly from the constants obtained by Scherer *et al.*,[6] as might be expected. The fact that the rotational constants found for the perturbing state are so different from those of other vibrational levels in the $\tilde{A}$ state indicates that the model used is not correct and that the $3\nu_3'$ and/or the perturbing state are probably perturbed by a third state. In conclusion we can say that although the assignment of some "extra" rotational lines has been changed, there is no need to change the proposed assignment[6] of the perturbing state as $\nu_2' + 2\nu_4'$.

### B. Singlet–triplet interactions

Due to a strong singlet–triplet interaction every rotational level in the electronically excited $\tilde{A}$ state is split into several components, the so-called molecular eigenstates. These molecular eigenstates, $|ME\rangle$, can be described as a linear combination of a zero-order $\tilde{A}$ state singlet level, $|S_1\rangle$, and zero-order triplet states, $|T_i\rangle$:

$$|ME\rangle = C_S|S_1\rangle + \sum_{i=1}^{n} C_{T_i}|T_i\rangle. \tag{1}$$

In order to deduce the zero-order singlet and triplet states, the density of coupled triplet states, $\rho_T$, and the singlet–triplet coupling matrix elements, $V_{ST}$, from the observed spectra we adopt the deconvolution procedure of Lawrance and Knight.[15] This method is in principle only applicable to a spectrum with known absorption intensities, whereas we have measured the laser-induced fluorescence excitation spectrum. It can be shown that the absorption intensity of the molecular eigenstate is proportional to the intensity of the molecular eigenstate in the LIF excitation spectrum in the case where the decay rates of the zero-order triplet states are negligible with respect to the decay rate of the zero-order singlet state.[16]

It is well known that the radiative decay rates of triplet states in acetylene are much smaller than the radiative decay rate of the $\tilde{A}$ singlet state.[17] A comparison of our excitation intensities with the lifetime measurements by Ochi and Tsuchiya[11] shows that for the $3_0^3$ and $2_0^1 4_0^2$ vibronic bands the absorption intensities are proportional to the excitation intensities. A comparison of both experiments for the $3_0^4$ band shows that this not the case for this vibronic band, indicating that the decay rates of the triplet states are no longer negligible. Fluorescence yield measurements[18] and lifetime measurements[19] have shown that the $4\nu_3'$ level predissociates and that indeed triplet states are involved in this predissociation. Yet, we assume for our deperturbation analysis that for all three vibrational levels the excitation and absorption intensities are equal, since no information on the lifetimes of the individual molecular eigenstates is available. With this assumption we are now able to deconvolute the spectra into zero-order singlet and triplet states. The results of the deconvolution procedure for the three vibrational levels, $3\nu_3'$, $4\nu_3'$, and $\nu_2' + 2\nu_4'$, are listed in Tables I and II.

The density of coupled triplet states, $\rho_T$, can be defined from the set of coupled zero-order triplet states as

$$\rho_T = \frac{n-1}{\Delta E}. \tag{2}$$

Here $n$ is the number of coupled zero-order triplet states and $\Delta E$ is the energy difference between the highest and lowest energy zero-order triplet state. Using this expression the density of coupled triplet states has been determined for every individual rotational level. The results can be found in Table II.

It can be seen from from Table II that for the $3\nu_3'$ and $4\nu_3'$ levels the average interaction coupling matrix elements $\langle V_{ST}\rangle$ do not systematically depend on the rotational quantum number $J$. This indicates that no Coriolis-induced intersystem crossing is present in acetylene. The average coupling strengths for the $3\nu_3'$ and $4\nu_3'$ are found to be 1281 and 823 MHz, respectively. The small decrease in the coupling constant can be attributed to a diminishing Franck–Condon overlap between the singlet states and the vibronically excited triplet states. In order to determine whether the vibrational states in the triplet state are completely mixed, in which case an averaging of the coupling strength is expected, we have calculated the number:

$$\frac{1}{n}\sum_{i=1}^{n}\frac{(V_{ST}-\langle V_{ST}\rangle)^2}{\langle V_{ST}\rangle^2}. \tag{3}$$

This number amounts to 0.68 for the $3\nu_3'$ and to 0.49 for the $4\nu_3'$ state. We therefore conclude that the vibrational wave functions of the triplet states are only very weakly mixed and that the increase in vibrational excess energy results in a small additional mixing of the coupled triplet states.

For the $\nu_2' + 2\nu_4'$ level the coupling strength varies strongly with $J$. The variation in coupling strength appears to be proportional to the amount of $3\nu_3'$ character in this level, indicating that the coupling strength between the pure $\nu_2' + 2\nu_4'$ state and the triplet states is much smaller. This difference in coupling strength between the two vibrational levels at the same energy directly reflects the difference in Franck–Condon overlap between these two singlet states and the triplet states. An analysis of the vibrational modes involved shows that the Franck–Condon overlap is largest when the molecule tends to be linear.

As can be seen in Table II the density of coupled triplet states, $\rho_T$, depends on the rotational quantum number. For $J=1$ the number of coupled states is approximately a factor of 2 less than for $J\neq 1$. This difference in coupled triplet states arises from the selection rules involved in the singlet–triplet interaction. Since the coupling is induced by a spin–orbit interaction the following selection rules apply: $\Delta J=0$, $\Delta N=0,\pm 1$, and $\Delta K_a=0,\pm 1$. In order to deduce the density of triplet states, $\rho_T^v$ from the observed density of coupled states, $\rho_T$, these selection rules have to be taken into account. Since in the case of acetylene the rotational $A'$ constant is in the order of 10 $cm^{-1}$ only one out of the possible three $K$ levels is expected to interact with the singlet state. With these assumptions the density of triplet states is found to be $\rho_T^v = 4.9$ and $\rho_T^v = 6.3$ states/$cm^{-1}$ for the $3\nu_3'$ and $4\nu_3'$ vibrational level, respectively. These values differ considerably from those obtained by Zeeman anti-

TABLE IV. Calculated density of triplet states (states/cm$^{-1}$) for different electronic triplet states.

| Vibr. level | Electr. state | Energy[a] | Calc. density[b] | Obs. density |
|---|---|---|---|---|
| $3\nu_3'$ | $T_1\,^3B_2$ *cis* | 16 150 | 4.7 | 4.9 |
| | $T_1\,^3B_u$ *trans* | 13 950 | 2.6 | |
| | $T_2\,^3A_u$ *trans* | 10 450 | 1.0 | |
| | $T_2\,^3A_2$ *cis* | 7 750 | 0.3 | |
| $4\nu_3'$ | $T_1\,^3B_2$ *cis* | 17 150 | 6.0 | 6.3 |
| | $T_1\,^3B_u$ *trans* | 14 950 | 3.5 | |
| | $T_2\,^3A_u$ *trans* | 11 450 | 1.3 | |
| | $T_2\,^3A_2$ *cis* | 8 750 | 0.5 | |

[a]Energy difference (cm$^{-1}$) between the minimum of the potential energy surface of the triplet state and the vibrational level in the $\tilde{A}$ state.
[b]In the calculations the normal mode frequencies of the $\tilde{A}$ state are used (Ref. 24).

crossing (ZAC) spectroscopy,[10] where the density of coupled states for these vibrational levels was found to be more than 100 states/cm$^{-1}$. This density was explained by a coupling of the $|S_1\rangle$ states via the triplet states with high vibrational levels of the electronic ground state, $|S_0\rangle$. The coupling matrix elements between the triplet states and the $|S_0\rangle$ levels was found to be in the order of a few MHz. Since this coupling is so weak the $|S_0\rangle$ states cannot be observed with the resolution and signal-to-noise ratio in the present experiment. The observed density of coupled states is therefore fully determined by the density of triplet states this in contrast to the ZAC experiment.

*Ab initio* calculations have shown that two triplet states lie below the $\tilde{A}\,^1A_u$ state.[20–22] Both triplet states are expected to have minima in the *cis*- and *trans*-bent configurations. The calculated potential energy minima of these triplet states agree reasonably well with the few published experimental values.[17,23] In order to determine which triplet state is responsible for the observed intersystem crossing we have computed, by direct level count, the density of states at the energies of the $3\nu_3'$ and $4\nu_3'$ vibrational levels. Since only very little experimental information is available on the triplet states we have used in this calculation the normal mode frequencies of the $\tilde{A}$ state[24] and the potential energy minima calculated by Lischka and Karpfen.[22] In these computations we have ignored the vibrational selection rules imposed by the spin–orbit coupling. The results of the calculations are listed in Table IV.

Comparing the observed and computed densities of triplet states it is clear that only the $T_1\,^3B_2$ (*cis*) state can be responsible for the observed density of states, although it cannot be excluded that also other triplet states contribute. Another indication that the $T_1\,^3B_2$ (*cis*) state is involved in the perturbation is provided by the vibrational dependence of the coupling strength, i.e., the Franck–Condon overlap between the wavefunctions of the singlet and triplet states. As has been pointed out by Dupre *et al.*,[10] the Franck–Condon overlap between the wave functions of the *trans*-bent $\tilde{A}$ state and the *cis*-bent $T_1$ state is expected to be large when the molecule tends to be linear, especially in the neighborhood of the *cis–trans* isomerization barrier of the triplet state. This has indeed been observed. Hence, we conclude that the observed perturbations in the $3\nu_3'$ and $4\nu_3'$ vibrational levels in the $\tilde{A}\,^1A_u$ state of acetylene are due to a spin–orbit interaction with excited vibrational levels of the $T_1\,^3B_2$ (*cis*) state.

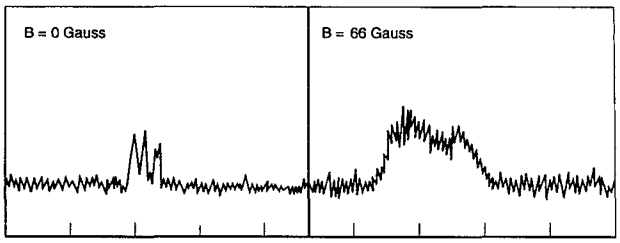


FIG. 2. Left panel: Recording of the $R(3)$ transition of the $3_0^3$ band at 45 309.0744 cm$^{-1}$ showing clearly three hyperfine components ($A_{\text{eff}}$=8.4 MHz). Right panel: The same transition recorded in a magnetic field of 66 Gauss.

### C. Hyperfine structure

The rotational levels in the $\tilde{A}\,n\nu_3'$ state with even $K_c$ quantum numbers have a total nuclear spin, $I=0$, whereas the rotational levels with odd $K_c$ quantum numbers have a total nuclear spin $I=1$. The nuclear spin $\mathbf{I}$ of these states may couple with the angular momentum $\mathbf{J}$ to form the resulting vector $\mathbf{F}=\mathbf{J}+\mathbf{I}$. For a $^1\Sigma$ state this coupling is very weak, in the order of a few kHz, and as a result the hyperfine structure of the $\tilde{A}$ state of acetylene, which corresponds to $^1\Sigma_u^-$ in $D_{\infty h}$, cannot be resolved with the present resolution. However, for triplet states this coupling is much stronger, in the order of 100 MHz. Due to the strong singlet–triplet interaction in acetylene the hyperfine structure of the triplet states becomes observable in the $\tilde{A}\leftarrow\tilde{X}$ excitation spectrum. Most of the molecular eigenstates involving rotational levels having a nuclear spin $I=1$ are split into three hyperfine components. This hyperfine splitting is usually largest for the weak lines, which are expected to have the largest amount of triplet character. Figure 2 shows an example of such a hyperfine splitting.

Comparing acetylene with other small hydrocarbons like glyoxal and propynal it can be expected that the hyperfine splitting in the triplet state is largely determined by the the Fermi contact parameter.[25,26] Assuming that the triplet states in acetylene can be represented by the ($b_{\beta J}$) coupling case the hyperfine structure of a rotational level in the triplet state is given by

$$\langle T|\hat{H}_{\text{HF}}|T\rangle = A_{\text{FC}}\frac{J(J+1)+S(S+1)-N(N+1)}{2J(J+1)} \times \tfrac{1}{2}\left[F(F+1)-J(J+1)-I(I+1)\right]. \quad (4)$$

Here $A_{\text{FC}}$ is the Fermi contact parameter, $N$ the angular momentum due to the rotational motion, $S$ the electron spin angular momentum and $\mathbf{J}=\mathbf{N}+\mathbf{S}$ the total angular momentum apart from nuclear spin.

The hyperfine structure of a molecular eigenstate is obtained by combining Eqs. (1) and (4) yielding:

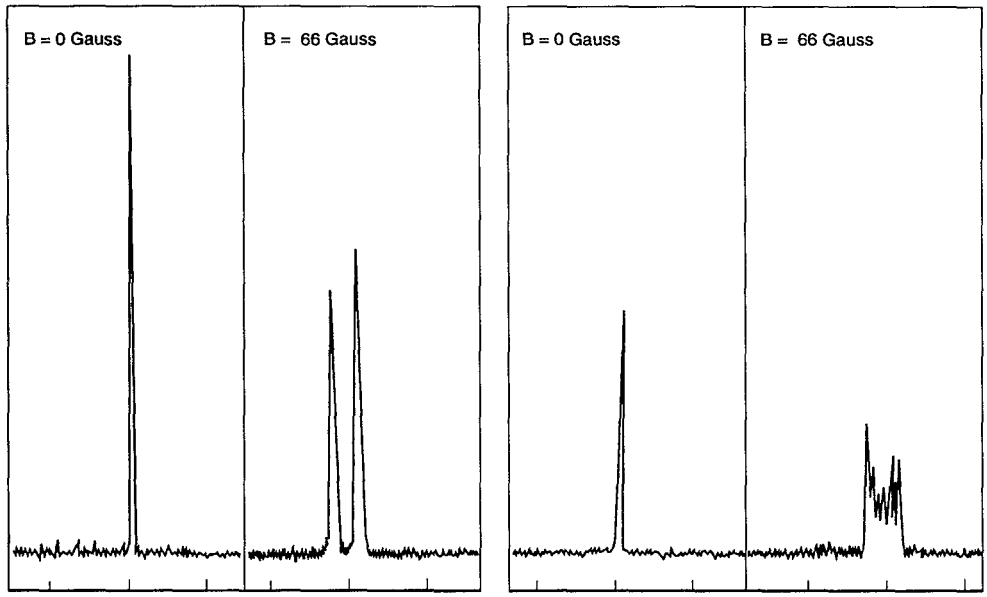


FIG. 3. Left panel: The $R(0)$ transition at 45 303.1653 $cm^{-1}$ at zero field and in a magnetic field of 66 Gauss. Only two components are observed, $M=-1$ and $M=+1$, due to selection rules. Right panel: The $R(2)$ transition at 46 294.2966 $cm^{-1}$ in a magnetic field of 0 and 66 Gauss. The seven $M$ sublevels can just be resolved.

$$\langle ME|\hat{H}_{\rm HF}|ME\rangle = \sum_{i=1}^{n} |C_{T_i}|^2 \langle T_i|\hat{H}_{\rm HF}|T_i\rangle$$
$$= A_{\rm eff}\frac{1}{2}\left[F(F+1)-J(J+1)-I(I+1)\right], \tag{5}$$

where $A_{\rm eff}$ is defined by

$$A_{\rm eff} = \sum_{i=1}^{n} |C_{T_i}|^2 A_{\rm FC}\frac{J(J+1)+S(S+1)-N(N+1)}{2J(J+1)}. \tag{6}$$

Here we have assumed that the $\hat{H}_{\rm HF}$ acts only on triplet states and is diagonal in $|T\rangle$. Unfortunately, our experiments give no information on the $N$ values of the coupled triplet states, except that $N$ is restricted to $N=J$, $J\pm1$. Therefore, it is not possible to determine directly the Fermi contact parameter $A_{\rm FC}$ from the observed spectra. Only the effective parameter $A_{\rm eff}$ can be determined for every individual eigenstate. The values found for this parameter can found in Table I.

By setting $N=J-1$ for every zero-order triplet state it is possible to determine a lower limit for $A_{\rm FC}$ from the effective values of the individual molecular eigenstates. For the triplet states probed via the $3\nu_3'$ level a lower limit of $A_{\rm FC}\geqslant 30$ MHz is found, whereas for the triplet states probed via the $4\nu_3'$ level a lower limit of $A_{\rm FC}\geqslant 50$ MHz is found. A more accurate value for $A_{\rm FC}$ can be obtained by comparing the effective hyperfine contact parameter $A_{\rm eff}$ with the effective gyromagnetic factor $g_{\rm eff}$ of a molecular eigenstate. This $g$ factor has been determined for all the individual lines by magnetic field measurements, see Sec. III D. Since $A_{\rm eff}$ and $g_{\rm eff}$ depend in the same way on the rotational quantum numbers of the triplet state, see also Sec. III D, the ratio $A_{\rm eff}/g_{\rm eff}$ is equal to the ratio $A_{\rm FC}/g_e$. Knowing that $g_e=2.0023$, the Fermi contact parameter can be determined to be $A_{\rm FC}=33\pm5$ MHz and $A_{\rm FC}=51\pm12$ MHz for the triplet states probed at the $3\nu_3'$ level and $4\nu_3'$ level, respectively. The value of 51 MHz for the $4\nu_3'$ level is in good agreement with the values determined by ZAC spectroscopy for other vibrational levels in the $\tilde{A}$ state.[8,27] The value of 33 MHz for the $3\nu_3'$ level is, however, considerably smaller than the value of 57.7 MHz determined via ZAC spectroscopy[8] for this vibrational level. The analysis of the singlet–triplet perturbations has shown that there is no substantial difference in the interaction of the $3\nu_3'$ and the $4\nu_3'$ vibronic levels with the triplet states which could have explained the observed difference. The small value of $A_{\rm FC}$ determined via the $3\nu_3'$ vibrational level in the present experiment therefore remains an enigma.

### D. Magnetic field measurements

To gain a better insight into the character of the coupled states we have studied the molecular eigenstates in the presence of a magnetic field. The interaction of zero-order singlet levels with a magnetic field is too weak to produce effects that can be resolved with the present resolution. Therefore, the magnetic field effects that are observed have to be attributed to the interaction of zero-order triplet states with the magnetic field. The energy shift of a rotational level in a triplet state can, with the weak magnetic fields used in the present experiment, be described by the first-order Zeeman effect

$$\langle T|\hat{H}_Z|T\rangle = g_e\frac{J(J+1)+S(S+1)-N(N+1)}{2J(J+1)}\mu_B B M_J. \tag{7}$$

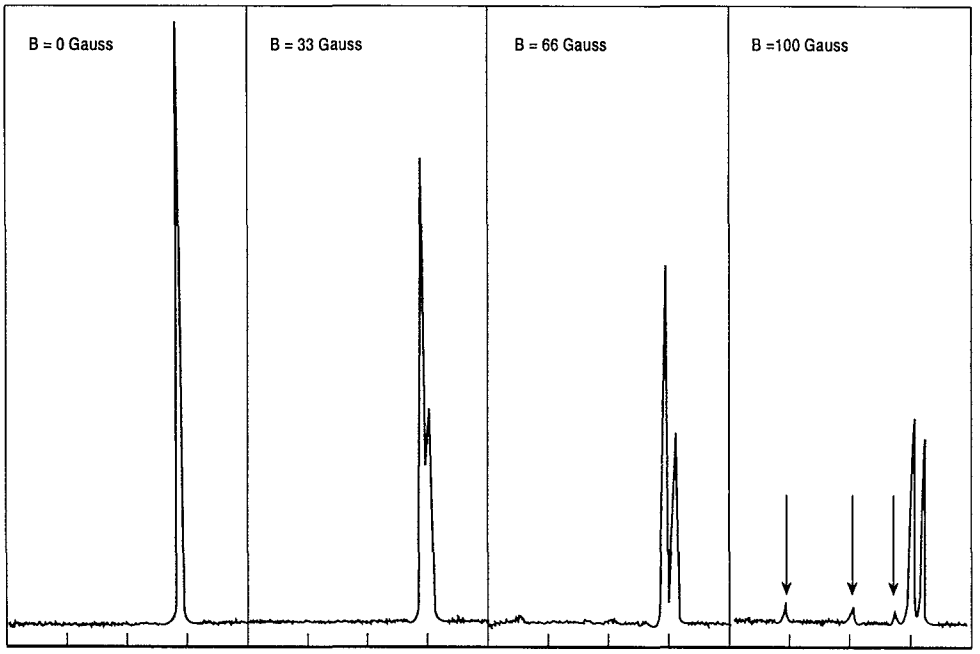


FIG. 4. Recording of the $R(0)$ transition of the $3_0^4$ vibronic band at 46 290.5047 $cm^{-1}$ in magnetic fields up to 100 Gauss. The arrows indicate the coupled $|S_0\rangle$ levels. The frequency is marked every 300 MHz and increases from right to left.

Here $g_e=2.0023$ is the gyromagnetic ratio, $\mu_B$ is the Bohr magneton, $B$ is the magnetic field strength, and $M_J$ is the projection of $J$ on the magnetic field. Just as in the case for the hyperfine structure only an effective $g_{\text{eff}}$ value can be determined from the observed spectra. The Zeeman splitting of the molecular eigenstate is given by

$$\langle ME|\hat{H}_Z|ME\rangle = g_{\text{eff}}\mu_B B M_J, \tag{8}$$

where $g_{\text{eff}}$ is defined as

$$g_{\text{eff}} = \sum_{i=1}^{n} |C_{T_i}|^2 g_e \frac{J(J+1)+S(S+1)-N(N+1)}{2J(J+1)}. \tag{9}$$

In the case where no hyperfine structure is present the lines in the spectrum show a Zeeman splitting in a magnetic field according to Eq. (8). Figure 3 shows two typical examples of such a splitting. The $g_{\text{eff}}$ values derived from these splittings are listed in Table I. The agreement between the values obtained in the present high resolution experiment and those found in the quantum beat experiment of Ochi and Tsuchiya[11] is striking.

However, if hyperfine structure is present, Eq. (7) is no longer valid and has to be replaced by an expression which also includes the hyperfine interaction. Since the structure of the lines in a magnetic field can not be fully resolved, as can be seen in Fig. 2, the Zeeman pattern cannot be exactly analyzed. We therefore decided to determine $g_{\text{eff}}$ from the total width of the lines assuming that the splitting can be treated in the high-field (Paschen–Back) limit. In this limit, Eq. (7) has to be replaced by

$$\langle T|\hat{H}_Z|T\rangle = g_e \frac{J(J+1)+S(S+1)-N(N+1)}{2J(J+1)} \times \mu_B B M_J + A_{\text{FC}} M_J M_I. \tag{10}$$

Here $A_{\text{FC}}$ is the Fermi contact parameter and $M_I$ the projection of the nuclear spin onto the magnetic field. Numerical calculations have shown that the error introduced by this assumption is in the order of 10%–20%, which is only slightly more than the error introduced by the uncertainty in the line splittings. The results of this analysis can be found in Table I.

All the molecular eigenstates studied in a magnetic field, except two, show a Zeeman splitting that can be fully explained by Eq. (8). If a weak magnetic field is applied the $R(0)$ $3_0^4$ $K_0^1$ transition at 46 290.5047 $cm^{-1}$ splits into two components, $M=-1$ and $M=+1$, as expected. When the magnetic field is increased some weak extra lines appear at higher energy and the intensity of the $M=+1$ component decreases dramatically, see Fig. 4. A similar effect is observed for the $R(3)$ $3_0^3$ $K_0^1$ transition at 45 308.9261 $cm^{-1}$. Also, here weak extra lines appear if a magnetic field is applied but in this case no dramatic loss in intensity is observed.

The extra lines that appear when a magnetic field is applied are most likely due to a magnetic field induced interaction of the molecular eigenstates with "dark" states. From the observed line positions and intensities the interaction strength can be estimated to be in the order of 10 MHz. Although it is difficult to determine the density of coupled "dark" states from the present observations, it can be estimated to be more than 100 states/$cm^{-1}$. Both the high density of coupled states and the value for the inter-

action strength indicate that the "dark" states are high-lying vibrational levels of the electronic ground state, $|S_0\rangle$. In principle, the $|S_0\rangle$ levels are observable around every molecular eigenstate. The observation of these states is, however, limited by the experimental linewidth and signal-to-noise ratio in our experiment. Consequently, only those $|S_0\rangle$ levels that have a relatively strong interaction with a molecular eigenstate can be observed.

Due to the interaction between the molecular eigenstate and the dark $|S_0\rangle$ levels the intensity of the molecular eigenstate is distributed over the $|S_0\rangle$ levels. However, for the $R(0)$ $3_0^4$ transition the intensity gained by the $|S_0\rangle$ levels is smaller than the intensity loss of the molecular eigenstate. This indicates that the coupled $|S_0\rangle$ levels have a relatively large nonradiative decay rate. In order to check the validity of this hypothesis it is necessary to perform lifetime measurements on the molecular eigenstate and the individual $|S_0\rangle$ levels. Unfortunately, this is not possible with the present experimental setup. However, lifetime measurements on this rotational level performed with a broadband laser have shown that the lifetime of this level indeed decreases when a magnetic field is applied.[19] Hence, it can be concluded that the coupled ground state levels indeed have a relatively large nonradiative decay rate. However, it is not possible to decide on ground of these observations what kind of nonradiative processes are taking place. But, since the probed levels are above the theoretically[28–30] and experimentally determined[18,31,32] dissociation limit of acetylene it is very likely that the $|S_0\rangle$ levels predissociate. This implies that one possible pathway for the predissociation of acetylene is a coupling of $\tilde{A}$ state rovibronic levels via the $T_1\,^3B_2$ state with predissociating vibrational levels of the electronic ground state. A similar mechanism has been suggested by Satyapal and Bersohn[33] in order to explain the results obtained in their photodissociation experiments.

For the $R(3)$ $3_0^3$ transition the intensity gain of the $|S_0\rangle$ levels equals the loss of intensity of the molecular eigenstate. This implies that no fast nonradiative processes like predissociation of the $|S_0\rangle$ take place. On ground of this and the above-mentioned observations it can be concluded that the dissociation limit of acetylene lies between 45 330.4 and 46 290.5 $cm^{-1}$, in agreement with most theoretical and experimental results.[18,28,30–32]

## IV. SUMMARY

Laser-induced fluorescence spectra of the $3_0^3\,K_0^1$ and $3_0^4\,K_0^1$ vibronic bands of the $\tilde{A}\,^1A_u \leftarrow \tilde{X}\,^1\Sigma_g^+$ transition of acetylene have been recorded in a molecular beam with a resolution of 18 MHz. Each rotational transition appears to consist of a group of lines due to an interaction with isoenergetic triplet states. From the deconvolution of the excitation spectrum the singlet–triplet coupling matrix elements and the density of coupled triplet states have been determined. The singlet–triplet coupling elements are found to be in the order of 1 GHz for both vibrational levels. Comparison of the observed density of coupled triplet states with the calculated density of several low-lying triplet states shows that the $T_1\,^3B_2$ state is involved in the perturbation of the $\tilde{A}\,^1A_u$ state.

The Fermi interaction between the $3\nu_3'$ and $\nu_2' + 2\nu_4'$ vibrational level has been reinvestigated. Although some of the rotational transitions have been reassigned the conclusions drawn by Scherer *et al.*[6] are still valid.

Magnetic field measurements have shown that most of the lines in the excitation spectrum have large magnetic moments, confirming that the states involved in the perturbation are indeed triplet states. Furthermore, the magnetic field measurements have shown that the triplet states can also couple to high-lying vibrational levels of the electronic ground state. The coupling constants for this interaction are found to be in the order of several MHz. Evidence has been found that some electronic ground state vibrational levels predissociate at an excess energy of 46 290 $cm^{-1}$. This implies that the $\tilde{A}$ state of acetylene can predissociate by coupling via triplet states to these predissociating vibrational levels of the electronic ground state.

The Fermi contact parameter of the triplet states involved in the interaction with the $\tilde{A}$ state has been determined from the hyperfine structure observed in the excitation spectrum and the $g$ factor found by the magnetic field measurements and is in reasonable agreement with the values determined by Zeeman anticrossing spectroscopy.

## ACKNOWLEDGMENT

This research was made possible by the financial support of the Dutch Organization for Fundamental Research of Matter (FOM).

[1] C. K. Ingold and G. W. King, J. Chem. Soc. 2702 (1953).
[2] K. K. Innes, J. Chem. Phys. **22**, 863 (1954).
[3] J. K. G. Watson, M. Herman, J. C. van Craen, and R. Colin, J. Mol. Spectrosc. **95**, 101 (1982).
[4] J. C. van Craen, M. Herman, R. Colin, and J. K. G. Watson, J. Mol. Spectrosc. **111**, 185 (1985).
[5] J. C. van Craen, M. Herman, R. Colin, and J. K. G. Watson, J. Mol. Spectrosc. **119**, 137 (1986).
[6] G. J. Scherer, Y. Chen, R. L. Redington, J. L. Kinsey, and R. W. Field, J. Chem. Phys. **85**, 6315 (1986).
[7] E. Abramson, C. Kittrell, J. L. Kinsey, and R. W. Field, J. Chem. Phys. **76**, 2293 (1982).
[8] E. Abramson, Ph.D. thesis, MIT, Cambridge, MA 1985.
[9] N. Ochi and S. Tsuchiya, Chem. Phys. Lett. **140**, 20 (1987).
[10] P. Dupre, R. Jost, M. Lombardi, P. G. Green, E. Abramson, and R. W. Field, Chem. Phys. **152**, 293 (1991).
[11] N. Ochi and S. Tsuchiya, Chem. Phys. **152**, 319 (1991).
[12] W. A. Majewski and W. L. Meerts, J. Mol. Spectrosc. **104**, 271 (1984).
[13] J. Cariou and P. Luc, *Atlas de spectroscopie d'absorption de la molecule tellure* (CNRS, Paris, 1980).
[14] K. F. Palmer, M. E. Michelson, and K. N. Rao, J. Mol. Spectrosc. **44**, 131 (1972).
[15] W. D. Lawrance and A. E. W. Knight, J. Phys. Chem. **89**, 917 (1985).
[16] W. M. van Herpen, W. L. Meerts, K. E. Drabe, and J. Commandeur, J. Chem. Phys. **86**, 4396 (1987).
[17] H. R. Wendt, H. Hipler, and H. E. Hunziker, J. Chem. Phys. **70**, 4044 (1979).
[18] M. Fujii, A. Haijima, and M. Ito, Chem. Phys. Lett. **150**, 380 (1988); A. Haijama, M. Fujii, and M. Ito, J. Chem. Phys. **92**, 959 (1990).
[19] Y. Chen, D. M. Jonas, C. E. Hamilton, P. Green, J. L. Kinsey, and R. W. Field, Ber. Bunsenges. Phys. Chem. **92**, 329 (1988).
[20] R. W. Wetmore and H. F. Schaefer III, J. Chem. Phys. **69**, 1648 (1978).

[21] M. Peric, R. J. Buenker, and S. D. Peyerimhoff, Mol. Phys. **53**, 1177 (1984).
[22] H. Lishka and A. Karpfen, Chem. Phys. **102**, 77 (1986).
[23] J. M. Lisy and W. Klemperer, J. Chem. Phys. **72**, 3880 (1979).
[24] J. Vander Auwera, T. R. Huet, M. Herman, C. Hamilton, J. L. Kinsrey, and R. W. Field, J. Mol. Spectrosc. **137**, 381 (1989).
[25] M. Lombardi, R. Jost, C. Michel, and A. Tramer, Chem Phys. **57**, 341 (1981).
[26] H. Bitto, M. P. Docker, P. Schmidt, and J. R. Huber, J. Chem. Phys. **92**, 187 (1990).
[27] P. Dupre, Ph.D. thesis, L'Université Joseph Fourier, Grenoble, 1992.
[28] J. A. Montgomery, Jr. and G. A. Petersson, Chem. Phys. Lett. **168**, 75 (1990).
[29] Y. Osamura, F. Mitsuhashi, and S. Iwata, Chem. Phys. Lett. **164**, 205 (1989).
[30] C. W. Bauschlicher, Jr., S. R. Langhoff, and P. R. Taylor, Chem. Phys. Lett. **171**, 42 (1990).
[31] A. M. Wodtke and Y. T. Lee, J. Phys. Chem. **89**, 4744 (1985).
[32] D. P. Baldwin, M. A. Buntine, and D. W. Chandler, J. Chem. Phys. **93**, 6578 (1990).
[33] S. Satyapal and R. Bersohn, J. Phys. Chem. **95**, 8004 (1991).